Journal of Nano Research *Online: 2009-02-06*
ISSN: 1661-9897, Vol. 5, pp 13-23
doi:10.4028/www.scientific.net/JNanoR.5.13

Gold Particle Size Determination on Au/TiO_2-CeO_2 Catalysts by Means of Carbon Monoxide, Hydrogen Chemisorption and Transmission Electron Microscopy

C. Guzmán[1], G. Del Angel[1]*, R. Gómez[1], F. Galindo[1], R.Zanella[2], G. Torres[3], C. Angeles-Chavez[4], and J.L.G. Fierro[5]

[1]Universidad Autónoma Metropolitana-Unidad Iztapalapa. Departamento de Química, Área de Catálisis, Av. San Rafael Atlixco No. 186, C.P. 09340, A.P 55-534. México D. F.
[2] Centro de Ciencias Aplicadas y Desarrollo Tecnológico, UNAM, Circuito exterior S/N, Ciudad Universitaria, C.P. 04510, A.P 70-186, Delegación Coyoacan, México D.F.
[3]Universidad Juárez Autónoma de Tabasco, DACB, Km.1 Carretera Cunduacan-Jalpa de Méndez, CP86690, A.P. 24, Cuanduacan Tabasco, México.
[4]Instituto Mexicano del Petróleo, Eje Central Lázaro Cárdenas No 152 ,México 07730, D.F
[5]Insituto de Catálisis y Petroleoquímica CSIC, Canto Blanco, 28049 Madrid Spain.
*gdam@xanum.uam.mx, Gloria.del.angel@hotmail.com (corresponding autor)

Received: January 12th, 2008; revised: September 18th, 2008; accepted: December 5th, 2008

Keywords: gold supported catalysts; titania-ceria supports; gold-titania-ceria catalysts; gold nanoparticles TEM characterization; gold nanoparticles CO chemisorption; gold nanoparticles hydrogen chemisorption.

Abstract: Au/TiO_2 and Au/TiO_2-CeO_2 catalysts were prepared by the sol-gel method and carbon monoxide, hydrogen chemisorption and TEM spectroscopy have been exploited to determine the size of gold particles. The gold nanoparticles (8.1 to 2.1 nm) were deposited by using the deposition-precipitation method. The XRD characterization shows the presence of anatase as the TiO_2 crystalline phase; while by XPS spectroscopy, the presence of Au°, Au_2O_3, Ce^{3+} and Ce^{4+} species co-existing in the Au/TiO_2-CeO_2 catalysts is shown. The characterizations by TPD-CO as well as by TPD-H_2 (temperature programmed desorption) showed that on catalysts containing cerium, the gold particle size can be determined with great accuracy by using these chemisorption methods. The gold particle size calculated from either the CO or H_2 thermodesorption values is in good agreement with that obtained by High Resolution Transmission Electron Microscopy (HRTEM) and Scanning Transmission Electron Microscopy (STEM) analyses. It was proposed that the TPD-CO and/or TPD-H_2 techniques could be helpful for the characterization of the gold particles by TEM; especially when the high contrast in the pictures of the supports containing CeO_2 prevents the particle size from being determined.

Introduction

Due to their potential application in heterogeneous catalysis, supported gold catalysts have recently received so much attention [1-7]. The activity shown by Au has been strictly related to the formation of gold particles which must be in the order of nanoparticles (2-8 nm). Among the different preparation methods to obtain Au nanoparticles supported on metallic oxides, the deposition-precipitation with urea has been reported as one of the most efficient methods [8-10]. This method allows the control of the size of the particles by varying different parameters in the course of the preparation. Particularly on gold supported on titania, it has been reported that the deposition-precipitation method allows the formation of gold nanoparticles smaller than 8 nm showing an efficient activity for the oxidative degradation of organic pollutants [11-12]. On the

other hand, noble metals supported on cerium oxide have been reported as catalysts showing important oxidative properties [13]. According to the aforementioned, the deposition of gold on the combined TiO_2-CeO_2 mixed oxides and the study of the formation of gold nanoparticles on such catalysts could be of great interest. The preparation of gold particles supported on mixed oxides could be an advanced contribution for the improvement of the oxidative properties of gold.

Usually the gold nanoparticles supported on metallic oxides are characterized by TEM since it is a practical technique which leads to determine the particle size with great accuracy. However, the determination of gold particles by TEM on supports containing CeO_2 is complicated since the CeO_2 dark contrast prevents the nanoparticles from being accurately detected. In such a case, the use of alternative methods to determine the metallic particle size can be helpful to support the TEM characterizations, where the CO and H_2 chemisorptions are highly recommended to be performed on select metals. The CO adsorption has been frequently used to determine the metallic particle size of noble metals; even on gold supported catalysts [14]; however, as far as we know, the hydrogen chemisorption has not been reported as a technique to determine the particle size on gold supported catalysts. In this work we proposed to carry out both the CO and H_2 chemisorptions; and the comparison of the particle size obtained by these methods with those obtained by TEM. The characterization of supports and gold supported catalysts was performed by nitrogen adsorption, ICP (Inductive Coupled argon Plasma-atomic emission spectroscopy), XRD, Raman and XPS spectroscopies as well as by STEM-EDX and HRTEM; and by CO-TPD and H_2-TPD techniques.

Experimental Section

Preparation of Supports

The titania (TiO_2) and doped titania (TiO_2-CeO_2) supports were synthesized by the sol-gel method. The preparation was as follows: to a three neck flask containing an ethanol/water solution (16:8 molar ratio), the appropriate amount of $Ce(NO_3)_3 \cdot 6H_2O$ (Strem Chemicals 99.9 % Ce) to obtain 2.5, 5.0, 7.5 and 10 wt% CeO_2 in the doped titania was added. Afterwards, 1 mol of titanium n-butoxide (Aldrich 97%) was added drop wise for 1 h. Then, the solution was maintained in reflux until the gel was formed. After gelling, the sample was dried in air at 373 K, increasing the temperature with a program rate of 2 K/min until the annealing temperature (673 K) was reached; and then it was maintained at this temperature for 4 h.

Catalyst preparation

The Au/TiO_2 and Au/TiO_2-CeO_2 were prepared by deposition-precipitation with urea [10]. To 5 g of support, 125 mL of an aqueous 4.2 x 10^{-3}M solution of $HAuCl_4$ (Aldrich 49 % Au) and urea (0.42M) were added; and a pH modification ranging from 1.0 to 8.0 was observed. The suspension was maintained at 80ºC with vigorous stirring for 16 h, in darkness. Afterwards, the suspension was centrifuged, washed, dried and calcined with air flow (50 mL/min) at 300ºC. After this treatment, gold is in the metallic state [9]. To avoid gold decomposition, the catalysts were stored in darkness in a desicator under vacuum. The Au content of the materials was determined by Inductively Coupled Argon Plasma-Atomic Emission Spectrometry (ICAP-AES). The nominal concentration of gold was 2.0 wt%.

Adsorption measurements

The BET specific surface area was carried out in an automatic Quantachrome Autosorb 3B instrument. The Nitrogen adsorption isotherms were carried out at 77 K; prior to the nitrogen adsorption, the samples were outgassed overnight at 573 K. The specific surface area was calculated from the adsorption isotherms by the BET equation and the mean pore size distribution by the BJH method.

X-ray diffraction (XRD)

The X-ray diffraction spectra were obtained with a SIEMENS D500 diffractometer with Cu Kα radiation and a graphite secondary bean monochromator. The intensities were obtained in the 2 theta ranges between 20 and 110º with a step of 0.05° and a measuring time of 0.5 s per point.

Raman spectroscopy

The Near-infrared Fourier-Transform Raman spectroscopic measurements were performed in a Thermo Nicolet ALMEGA dispersive Raman spectrometer equipped with a diode-pumped Nd:YAG laser with an emission wavelength of 1064 nm. The beam was doubly focused on a sample mounted on a capillary tube. The light scattered at 90° over the sample was focused on the entrance slit of a double monochromator; and detected by a Peltier-cooled photomultiplier attached to a phonon counter.

XPS spectroscopy

A VR Escalab 200R electron spectrometer equipped with hemispherical analyzer equipment was used for XPS studies. The spectrometer was operated in a constant pass mode; and a nonmonochromatized Mg-Kα ($h\nu$= 1253.6 eV, 1eV. 1.603 x10^9 J) X-ray Source operated at 10 mA and 12 kV. A PDP 11/04 computer (Digital Co.) was used to record and analyze the spectra. The intensities of the peaks were estimated by calculating the integral peak after subtracting an S-shaped background and fitting the experimental peak to a combination of Lorentzian/Gaussian lines of variable proportions. The binding energies (BE) were referenced to the Ti2p peak; whose BE was fixed at 458.5 eV.

Transmission Electron Microscopy (TEM)

High resolution Transmission Electro Microscoscopy (HRTEM) and Scanning Transmission Electro Microscopy (STEM) analyses of different samples were performed in a JEE-2200FS transmission electron microscope with an accelerating voltage of 200 kV. The microscope is equipped with a schottky –Type Field emission gun and an ultra high resolution (UHR) Configuration (Cs=0.5mm; Cc=1.1mm; point to point resolution= 0.19nm); and an in-column omega-type energy filter. STEM is particularly useful in studies of nanoparticles when a high angle annular dark field (HAADDF) detector, which collects electrons that undergo Rutherford scattering, is used. The images can be acquired where the intensity is approximately proportional to Z^2 (Z is the atomic number of the scattering atom). Therefore, elements with high Z produce higher intensities and white contrast images. The technique is used to disclose the presence of different chemical elements when they have a big difference in atomic numbers, as it was found in the supported catalysts. The samples were ground, suspended in isopropanol at room temperature and dispersed with ultrasonic agitation; then, an aliquot of the solution was dropped on a 3mm diameter carbon film supported on lacey copper grid.

The mean particle size (d_s) of the Au particles was calculated by means of the following equation: $d_s = \Sigma n_i d_i^3 \; / \; \Sigma n_i d_i^2$, where d_i is the diameter measured directly from the electron micrographs; and n_i is the number of particles having the diameter d_i.

Temperature Programmed Desorption of CO (TPD-CO)

The TPD-CO study was carried out in a CHEMBET-3000 apparatus equipped with a TCD detector. The sample (100 mg) was reactivated *in situ* under H_2 flow at 300 ºC for 1 h. Afterwards, the sample was cooled at room temperature and purged with a He flow for 15 min. Then, a 5%CO/95% He mixture flow was admitted and maintained for 1h. Afterwards, the sample was purged with a He flow during 15 min. Finally, the desorbed CO was recorded from room temperature to 300 ºC with a carrier flow of He of 10 mL /min by using a program rate of 10ºC/min. The gold particle size was calculated by assuming a CO/Au stoichiometry ratio of 1.0 and a gold atomic cross sectional area of 0.08696 nm^2 [14].

Temperature Programmed Desorption of H_2 (TPD-H_2)

The TPD-H_2 study was carried out in a CHEMBET-3000 apparatus equipped with a TCD detector. The catalyst (100 mg) was firstly treated under nitrogen flow at 300 ºC during 1h. Then, the sample was cooled at room temperature. Afterwards, the sample was heated at 300ºC under a $75N_2/25H_2$ mixture flow for 1 h; then the sample was cooled at room temperature and then purged with N_2 for 15 min. Finally, the TPD spectra were recorded by heating the catalyst from room temperature up to 500 ºC with a nitrogen flow of 10 mL/min by using a program rate of 10 ºC/min. The gold particle size was calculated by assuming a H/Au stoichiometry ratio of 1.0 and a gold atomic cross sectional area of 0.08696 nm^2.

Results and Discussion

The specific surface area and mean pore size diameter obtained for the various TiO_2 and TiO_2-CeO_2 supports were reported in Table 1. A positive effect of cerium on the specific surface area of the TiO_2-CeO_2 was obtained. In comparing with the bare TiO_2 solid, the BET area increases from 64 m^2/g to 71-137 m^2/g for the TiO_2-CeO_2 samples. The large surface on the TiO_2-CeO_2 mixed oxide could be due to a modification by the cerium nitrate on the hydrolysis-condensation reactions rates of the titanium alkoxide as has been reported recently in TiO_2-CeO_2 supports and [15,16] and Au/TiO_2-CeO_2 catalysts [17].

Table 1. Support characterization.

Catalyst	Pore diameter (mean size) (nm)	Specific surface area (m^2/g)
TiO_2	3.3	64
TiO_2-CeO_2 2.5	5.4	71
TiO_2-CeO_2 5.0	5.9	117
TiO_2-CeO_2 7.5	5.4	130
TiO_2-CeO_2 10.0	6.9	137

The XRD patterns for the Au/TiO_2 and Au/TiO_2-CeO_2 samples are shown in Fig 1. The spectra showed the characteristic peaks for the anatase in all the samples. None of the characteristic peaks for ceria were identified. The absence of peaks corresponding to cerium oxide could suggest a high substitution of Ti^{4+} by Ce^{4+} non measurable by XRD. However, since the atomic ratio of Ce^{4+} (80 pm) is higher than that of Ti^{4+} (61 pm), a wide substitution cannot be expected. The high proportion of cerium oxide that was not incorporated into the titania network can be present as very small cerium oxide conglomerates undetectable by XRD even at high cerium oxide contents. It must be noted that in the enlarged XRD spectra, the peaks corresponding to Au° (2θ= 38.18, 44.39,

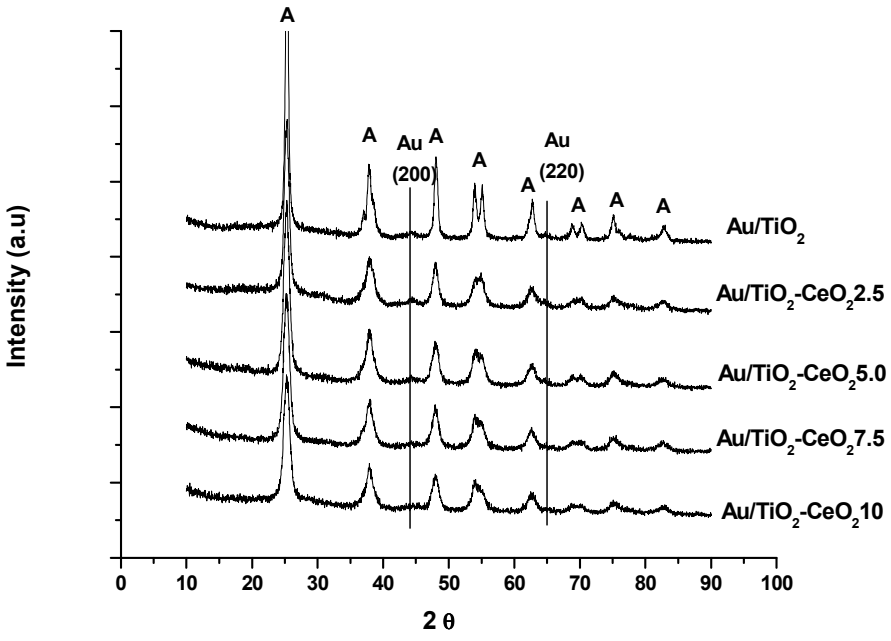

Figure 1. XRD-patterns for the Au/TiO_2 and Au/TiO_2-CeO_2 catalysts.

64.57) for the planes (111), (200) and (220), respectively, are not observed, which suggests that gold is present as nanozised-gold particles minor than 10 nm. The low Au content (2.0 wt %) in addition to the small size of the gold particles do not permit their detection by this technique. The elemental analysis, by ICAP-AES, showed gold contents on the catalysts around 2.0 - 2.1 wt%. The Raman spectra for the TiO_2 and TiO_2-CeO_2 samples in the 300-750 cm^{-1} region are presented in Fig. 2. The Raman spectra for the TiO_2 and TiO_2-CeO_2 catalysts show the peaks assigned to the anatase phase [18, 19]. A 4-cm^{-1} shift to higher energy peaks, 392 and 511 cm^{-1}, respectively, can be seen in the titania-cerium oxide semiconductor. The ≡Ti-O-Ti≡ energy bonds of the anatase phase are perturbed by the presence of cerium oxide, which suggests some substitutions of the Ti^{4+} by Ce^{4+} forming ≡Ti-O-Ce≡ bonds in the titania structure.

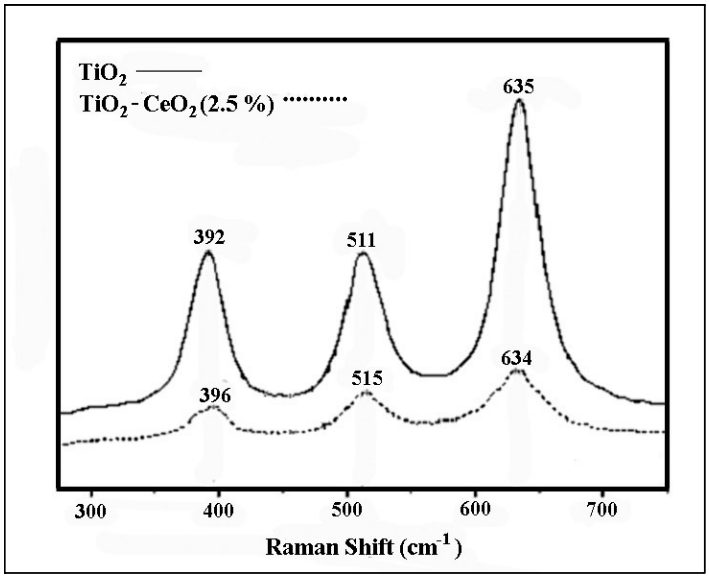

Figure 2. Raman spectra for the TiO_2 and TiO_2-CeO_2 supports.

The binding energies (BE) of the core and surface atomic ratios for Au, Ti and Ce are reported in Table 2. The binding energy $Au4f_{7/2}$ [20] for the Au/TiO_2-CeO_2 catalysts indicates that Au is present as Au° 83.8-84.0 eV; and as oxidized gold Au^+ 85.6 eV (Fig. 3) in proportions which are comprised between 74 to 87 % of reduced gold Au°. The presence of oxidized gold is probably due to the fact that the XPS spectra were obtained without previous treatment; and hence the formation of Au_2O_3 preferentially on the surface of the gold nanoparticles is expected. The preparation method by using urea as precipitant, then allows the formation of reduced gold [21, 22]. The $Ce3d_{5/2}$ binding energy [20] was also analyzed for select samples in the 870-920 eV region

Table 2. Binding energies (eV) and atomic ratio of the Au/TiO_2-CeO_2 catalysts.

Catalyst	Ti $2p_{3/2}$	O 1s	Au $4f_{7/2}$	$Ce3d_{5/2}$	Au/Ti at	Ce/Ti at
Au/TiO_2	458.6	529.9 (82)	83.8 (87)	-	0.026	-
		531.6 (18)	85.6 (13)			
Au/TiO_2-CeO_2 2.5	458.6	529.9 (80)	83.9 (77)		0.031	0.015
		531.5 (20)	85.7 (23)			
Au/TiO_2-CeO_2 5.0	458.5	529.9 (83)	83.9 (85)	Ce^{4+} (52)	0.025	0.024
		531.5 (17)	85.6 (15)	Ce^{3+} (48)		
Au/TiO_2-CeO_2 7.5	458.5	529.9 (81)	83.8 (74)	Ce^{4+} (49)	0.018	0.041
		531.4 (19)	85.6 (26)	Ce^{3+} (51)		
Au/TiO_2-CeO_2 10	458.5	529.9 (83)	84.0 (83)	Ce^{4+} (60)	0.017	0.063
		531.6 (17)	85.6 (17)	Ce^{3+} (40)		

(Fig. 4).The deconvoluted XPS spectra for the Au/TiO_2-CeO_2-7.5 sample showed the presence of Ce^{3+}/Ce^{4+} (881.9-886.2 eV) and Ce^{4+} (916.15 eV). The C^{4+}/Ce^{3+} relative abundance calculated from the areas of the deconvoluted spectra showed that oxidized $Ce^{4+}$and reduced Ce^{3+} species are almost in the same proportion (Table 2).

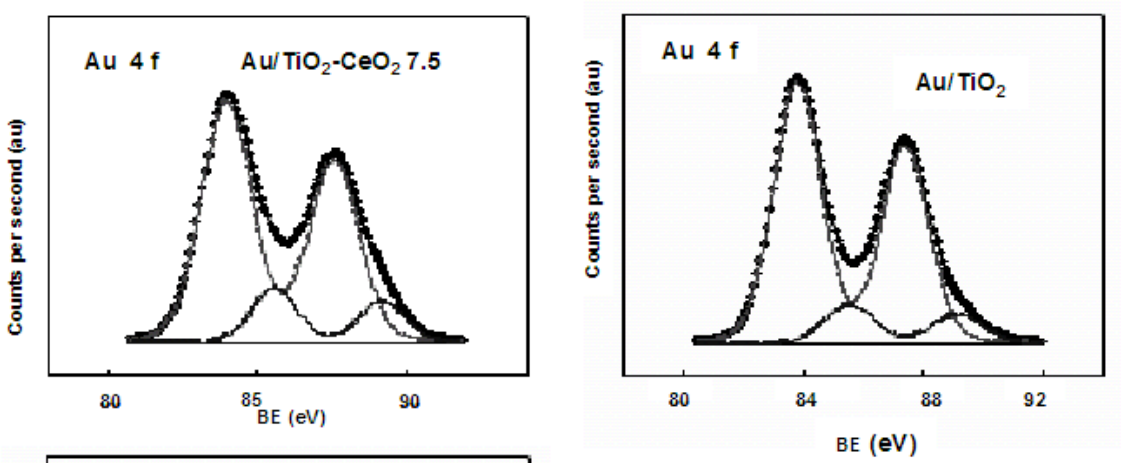

Figure 3. Au $4f_{7/2}$ core level spectra for the Au/TiO_2 and Au/TiO_2-CeO_2 catalysts.

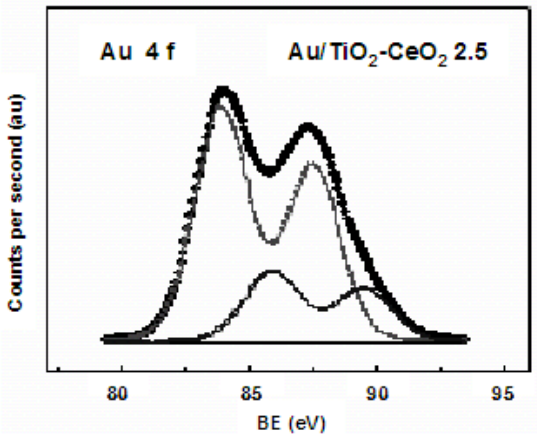

Figure 4. Ce 3d core level spectrum for the Au/TiO_2-CeO_2 catalyst.

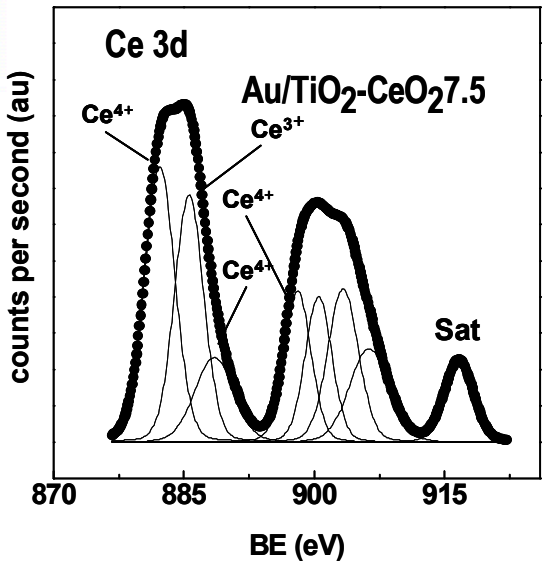

Fig. 5 shows the HRTEM images of different gold nanoparticles deposited on the TiO_2-CeO support. As it can be clearly seen, the nanoparticles typically presented the {1 1 1} and {2 0 0} planes that belong to the fcc metallic gold structure; and therefore they were oriented along the [0 1 1] direction. However, these gold nanoparticles presented different morphologies, generally five-fold symmetry twinned structures such as icosahedra and decahedra which tend to be slightly more stable in small sizes [23]. Particle size distributions were obtained form the Z contrast images; and they are presented in Fig. 6. The gold particles can be observed as small white spots which are in contrast with the support. More than 200 gold nanoparticles supported on the TiO_2-CeO_2 catalysts were counted and measured; the corresponding histograms are reported in Fig. 7. The obtained

values are reported in Table 3. The gold nanoparticles were found from 8.1 to 3.4 nm for Au/TiO_2 and Au/TiO_2-CeO_2-10 respectively. The particle size values are lower in the TiO_2-CeO_2 mixed oxides than that obtained on the Au/TiO_2 bare catalyst, which is 8.1 nm. The small particle size obtained on the TiO_2-CeO_2 catalysts prepared by the sol-gel method could be due to the high specific surface area obtained in these supports (Table 1).

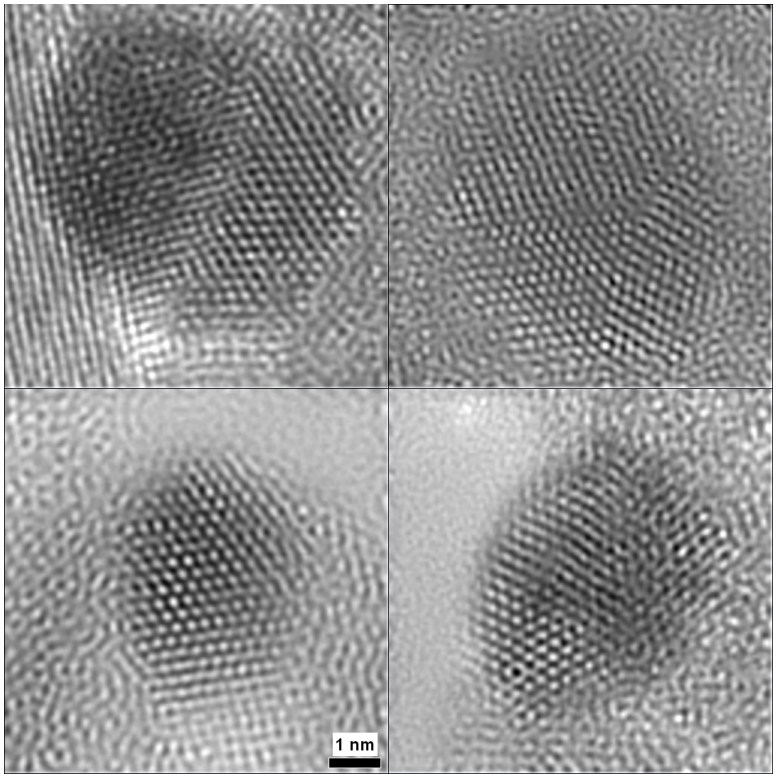

Figure 5. HRTEM image of gold nanoparticles with different morphologies oriented along the [0 1 1] direction for the Au/TiO_2-CeO_2-10 catalysts.

Table 3. Comparative results of the determination of the gold particle sizes on the sol-gel Au/TiO_2-CeO_2 catalysts.

Catalyst	[1]Au	TEM [2]ds	CO adsorption			H_2 adsorption		
			CO Chem	[3]D	[2]ds	H_2 Chem	[3]D	[2]ds
	(wt%)	(nm)	(μmol)	(%)	(nm)	(μmol)	(%)	(nm)
Au/TiO_2	2.0	8.1	15	15	8.0	5.3	10	11.0
$Au/TiO_2CeO_2$2.5	2.0	5.5	20	20	5.8	10.6	21	5.5
$Au/TiO_2CeO_2$5.0	2.1	3.7	30	28	4.2	16.1	29	4.0
$Au/TiO_2CeO_2$7.5	2.0	3.8	35	35	3.3	16.0	32	3.7
$Au/TiO_2CeO_2$10	2.1	3.4	37	37	3.2	19.0	35	3.3

[1]determined by ICAP-AES (inductive coupled argon plasma-atomic emission spectroscopy) [2]ds = mean particle size. [3]Dispersion

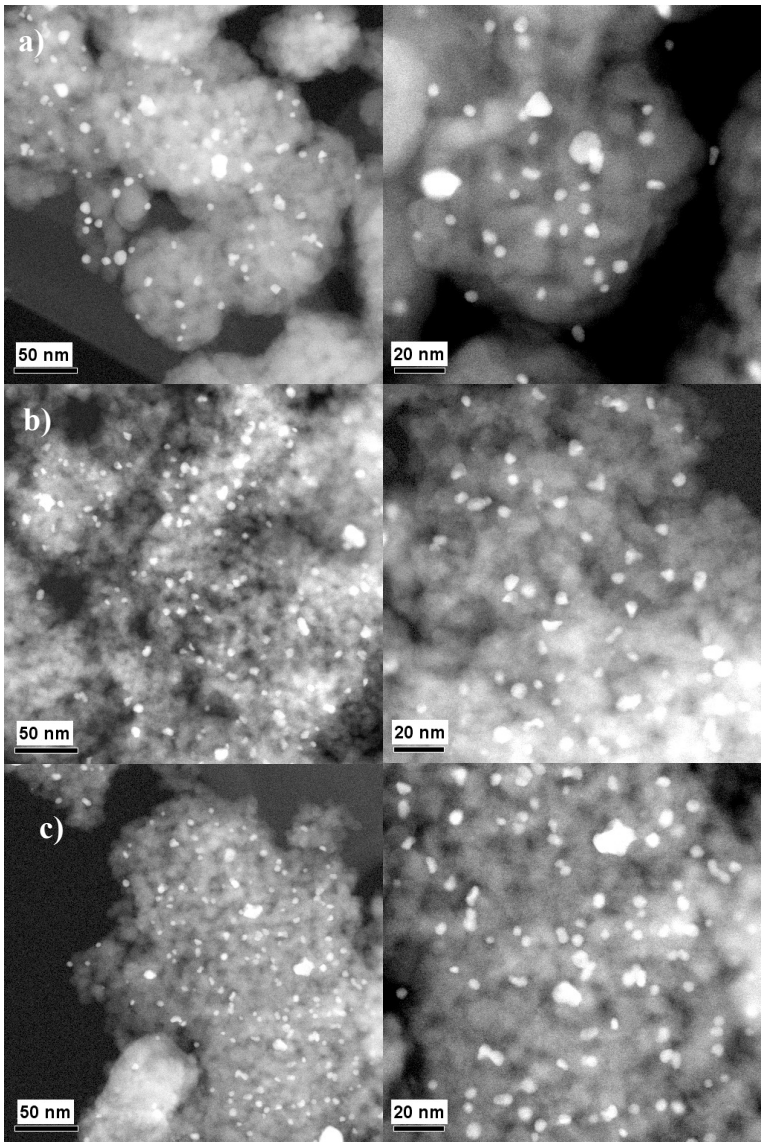

Figure 6. HAADF image for: a) Au/TiO_2, b) Au/TiO_2-$CeO_2$5 and c) Au/TiO_2-$CeO_2$10.

On the other hand, as it was mentioned before, the gold TPD-CO thermograms were obtained and analyzed to reveal the CO chemisorption behavior on the Au/TiO_2-CeO_2 catalysts. The corresponding TPD-CO thermograms presented in Fig. 8 showed a single peak for the CO desorption at temperatures lower than 100ºC in all the catalysts. As for the Au/TiO_2 catalyst, the desorption peak appears at 48ºC, whereas the desorption temperature for the Au/TiO_2-CeO_2 catalysts ranged from 57 to 66ºC. It can be seen that the shift of the CO desorption appears as a function of the cerium oxide content. The higher the cerium content, the higher the desorption temperature is. It has been reported that TiO_2 [24] and CeO_2 [14] adsorb CO and, therefore the TPD-CO determinations were carried out on the TiO_2 and TiO_2-CeO_2 supports at the identical conditions for the CO adsorption-desorption cycle used for the Au/TiO_2-CeO_2 catalysts. As for the supports, a remarkable CO desorption in the same range of temperatures as that observed for the Au supported catalysts (40 – 75ºC) was obtained (Table 3). The CO adsorbed on the TiO_2-CeO_2 supports has been related to the CO adsorbed on the reduced Ce^{3+} sites [25] and on the TiO_2 vacancies [24]. To obtain the CO uptake corresponding to the Au particles, the amount adsorbed on the support was subtracted from that chemisorbed on the Au supported catalysts. In Table 3, the gold particle size calculated by this method (CO/Au=1) is reported for the different catalysts. It can be seen that the gold particle size decreases as the amount of CeO_2 in the catalysts does. By comparing the Au nanoparticles calculated from the CO chemisorption values (8.0 to 3.2 nm) with those obtained from the TEM micrographs (8.1 to 3.4 nm), we found a plausible agreement between both techniques on Au/TiO_2-CeO_2 catalysts.

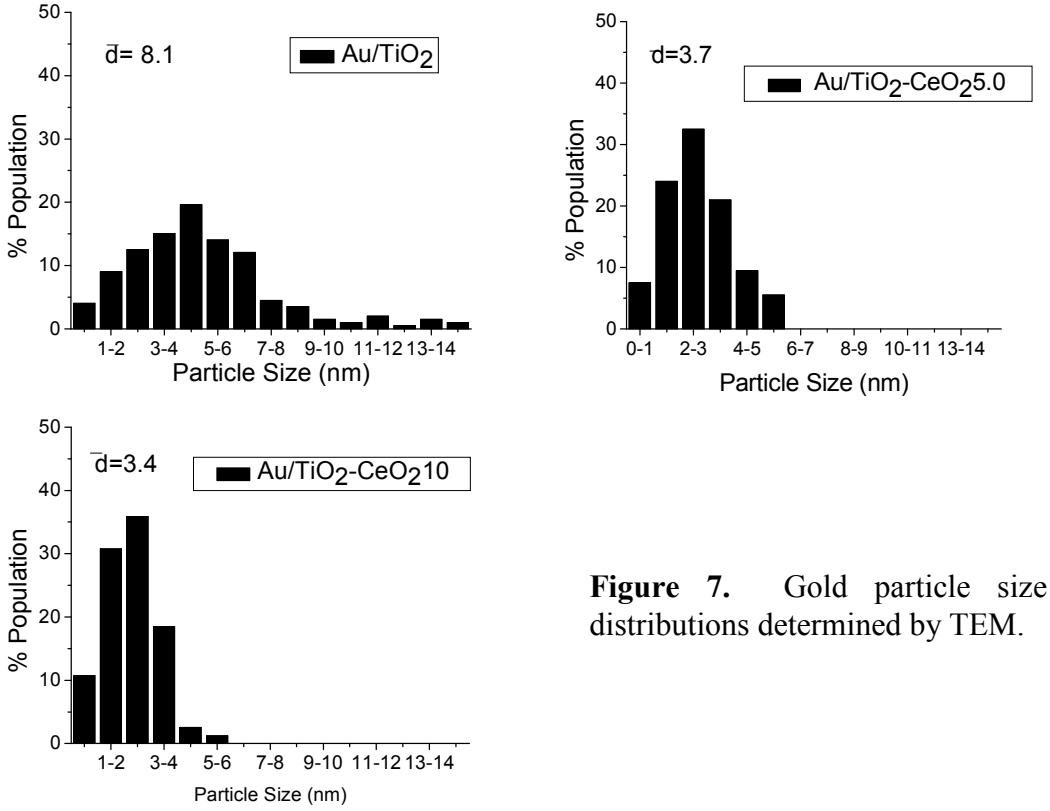

Figure 7. Gold particle size distributions determined by TEM.

The determination of the size of the Au nanoparticles by TPD-H_2 on the Au/TiO_2-CeO_2 catalysts presents some problems since the CeO_2 can also adsorb hydrogen. To avoid this problem, the catalysts were pre-treated at 300°C under hydrogen flow before carrying out the hydrogen desorption as it was mentioned in the experimental section. Under such pre-treatment conditions it could be assumed that the consumption of hydrogen by cerium oxide was saturated.

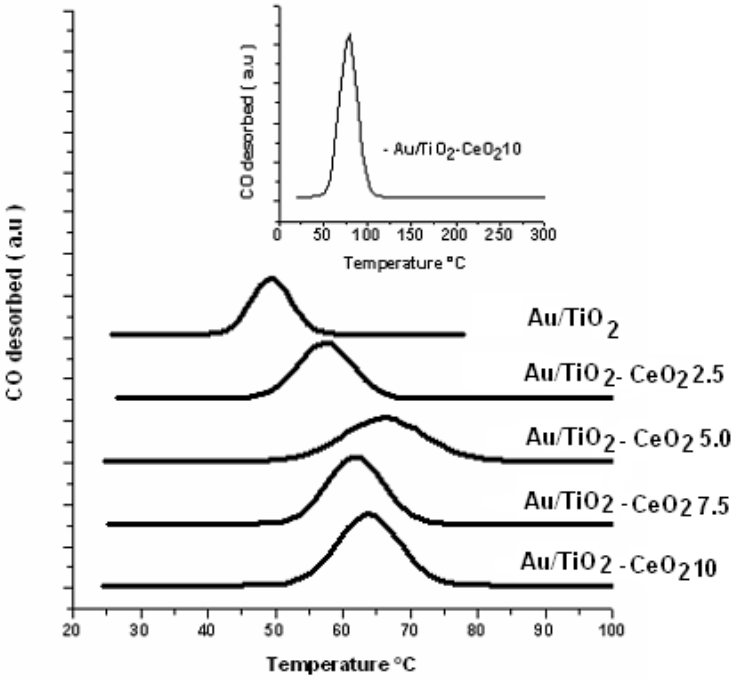

Figure 8. Temperature programmed desorption (TPD-CO) for the Au/TiO_2 and Au/TiO_2-CeO_2 catalysts.

In Fig. 9 the hydrogen desorption peaks at low temperatures 40-100°C for the various catalysts are shown. We assume then that the hydrogen desorbed in the temperature range of 40-100°C is the corresponding to hydrogen adsorbed on the gold atoms. A TPD-H_2 thermogram ranging from room temperature to 500°C was inserted in Fig. 9. The absence of additional desorption peaks between 100°C and 500°C indicates that on the reduced cerium oxide the hydrogen desorption from cerium oxide did not occur at temperatures below 500°C. The gold particle size calculated from the hydrogen desorbed (H/Au=1); and the mean particle size calculated by TPD-CO and TEM are reported in Table 3. The accuracy among the three techniques is highly reasonable.

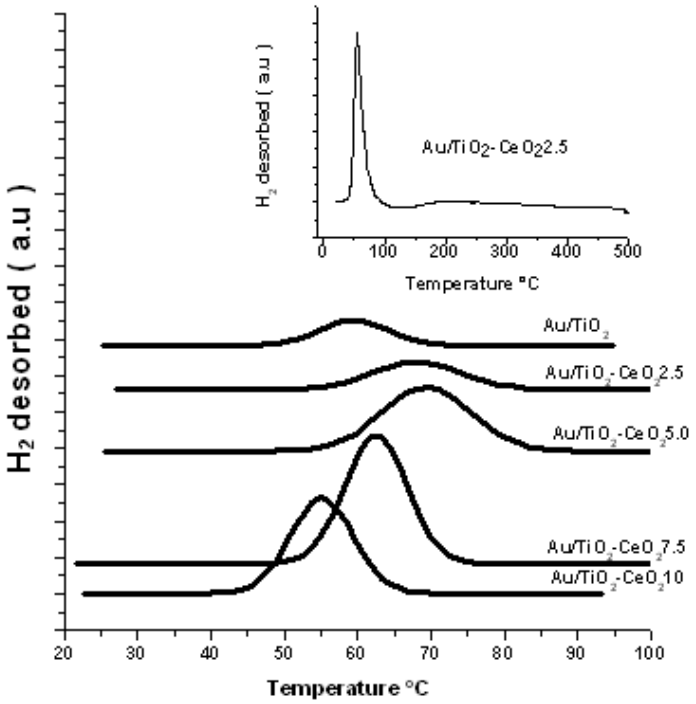

Figure 9. Temperature programmed desorption (TPD-H_2) for the Au/TiO_2 and Au/TiO_2-CeO_2 catalysts.

Conclusions

On the TiO_2-CeO_2 sol-gel supports with different CeO_2 contents (2.5, 5.0 7.5 and 10 wt% CeO_2), gold nanoparticles deposited by the deposition-precipitation with urea were obtained. A positive effect of cerium oxide on the specific surface areas of the supports was observed. The BET area was increased from 64 m^2 on the TiO_2 bare support to 137 m^2/g on the TiO_2-CeO_2 supports. It was found that the size of the supported gold nanoparticles can be estimated from the TPD-CO and TPD-H_2 thermograms. The particle size ranged from 8.0 to 3.2 nm for carbon monoxide, whereas that of hydrogen ranged from 11.0 to 3.3 nm. On the other hand, the particle size determined by chemisorption; and that estimated from TEM (8.1 to 3.4 nm) were almost on the same range; then a good accuracy between both techniques was obtained. It is proposed that the CO and H_2 chemisorption studies could help to the TEM characterizations especially when the high contrast of titania and cerium oxide prevents the size of the gold nanoparticles from being determined.

Acknowledgements
We acknowledge CONACYT for the support provided to the Project SEP-CONACYT 2004-COI-46689Q. C. Guzmán thanks CONACYT for the grants awarded.

References

[1] M. Haruta and M. Date, Appl. Catal. A: General Vol. 222 (2001), p. 427
[2] M. Haruta, Cattech Vol. 6 (2002), p. 102
[3] D.A.Bulushev, Dimitri, I. Yuranov, E.I. Suruvova, P.A. Buffat, and L. Kiwi-Minsker, J. Catal. Vol. 224 (2004), p. 8
[4] G.C. Bond and D.T. Thompson, Gold Bull. Vol. 33 (2000), p. 41
[5] K. Ki-Joong, Y. Young-Jae, C. Min-Chul, K. Chan-Soon, C. Kyong-Hwan, S. Woon-Jo, J. Seung-Won, and A. Hogeun, J. Nanosci. Nanotechnol. Vol. 6 (2006), p. 3589
[6] R. Esparza, J.A. Ascencio, G. Rosas, J.F. Ramírez, U. Pal, and R. Perez, J. Nanosci. Nanotechnol. Vol. 5 (2005), p. 641
[7] E. Smolentseva, N. Bogdanchikova, A. Simakov, A. Pestryakov, M. Avalos, M.H. Farias, A. Tompos, and V. Gurin, J. Nanosci. Nanotechnol. Vol. 7 (2007), p. 1882
[8] M. Haruta, J. Catal. Vol. 36 (1997), p. 153
[9] M. Haruta, S. Tsubota, T. Kobayashi, H. Kageyama, M.J. Genet, and B. Delmon, J. Catal. Vol. 144 (1993), p. 175
[10] R. Zanella, S. Giorgio, S. Chae-Ho, C. R. Henry, and C. Louis, J. Catal. Vol. 222 (2004), p. 357
[11] M. Besson, A. Kallel, P. Gallezot, R. Zanella, and C. Louis, Catal. Comm. Vol. 4 (2003), p. 471
[12] A.C. Gluhoi, N. Bogdanchikova, and B. E. Nieuwenhuys, J. Catal. Vol. 229 (2005), p. 154
[13] R. Taha, D. Duprez, N. Mouaddib-Moral, and C. Gauthier, Stud. Surf. Sci. Catal. Vol. 116 (1998), p. 549
[14] U.R. Pillai and S. Deevi, Appl. Catal. A: General Vol. 299 (2006), p. 266
[15] T. López, F. Rojas, R. Alexander-Katz, F. Galindo, A. Balankin, and A. Buljan, J. Solid State Chem. Vol. 177 (2004), p. 1873
[16] F. Galindo, R. Gomez, and M. Aguilar, J. Mol. Catal A Chemical, doi10.1016/jmolcata.200710.08.
[17] X. Bokhimi and R. Zanella, J. Phys. Chem. C Vol. 111 (2007), p. 2525
[18] Mineral Raman DataBase, Laboratory of Photoinduced Effects, Vibrational and X Spectroscopies - PHEVIX, Dipartimento di Fisica, Università degli Studi di Parma, Italy, http://www.fis.unipr.it/phevix/ramandb.html.
[19] B. Liu, X. Zhao, N. Zhang, Q. Zhao, X. He, and J. Feng, Surf. Sci. Vol. 595 (2005), p. 203.
[20] Handbook of X-Ray Photoelectron Spectroscopy, by G.E. Mulillenberg (Editor), Perkin-Elmer Corporation, Phisycal Electronics division, USA (1978).
[21] R. Zanella and C. Louis Catalysis Today, Vol. 107-108 (2005), p. 768
[22] L. Delannoy, N. Weiher, N Tsaptsaris, A. M. Nachari , S. Luanga, L. M. Sven, C. Louis, Top in Catal, Vol. 44 (2007), p. 263.
[23] J. L. Elechiguerra, J. Reyes-Gasga, M. J. Yacaman, J. Mater. Chem. Vol. 16 (2006), p. 3906
[24] F. Boccuzzi, A. Chiorino, M. Manzoli, P. Lu, T. Akita, S. Ichikawa, M.Haruta, J. Catal. Vol. 202 (2001), p. 256
[25] F.A. Bonzon-Verduraz, A. Bensalem, J. Chem. Soc. Faraday Trans. Vol. 90 (1994), p. 653